Journal homepage: http://gwse.iheg.org.cn

Numerical modelling of the dynamic process of oil displacement by water in sandstone reservoirs with random pore structures

Fei Gao[1], Feng Liu[2,3,4], Hua-jun Wang[1*]

[1] *School of Energy and Environment Engineering*, *Hebei University of Technology*, *Tianjin* 300401, *China*.
[2] *Institute of Hydrogeology and Environment Geology*, *Chinese Academy of Geological Sciences*, *Shijiazhuang* 050061, *China*.
[3] *Technology Innovation Center of Geothermal & Hot Dry Exploration and Development*, *Ministry of Natural Resources*, *Shijiazhuang* 050061, *China*.
[4] *China University of Geosciences(Beijing)*, *Beijing* 100000, *China*.

Abstract: In order to maintain the production rate of a reservoir and improve the displacement efficiency, it is crucial to have an in-depth understanding of the process of oil displacement by water. However, with respect to the conceptualization of porous media of a reservoir, very limited efforts have been made to the pore structures inside the reservoirs. In this paper, the pore structures of a sandstone reservoir were generated by using the method of random growth algorithm. Based on the randomly generated model, a theoretical model to describe the dynamic process of oil displacement by water in the sandstone reservoir was established, and then corresponding numerical modelling was performed. The effects of the displacement velocity, the viscosity ratio of oil-water phase and the porosity of reservoirs on the displacement performance were also analyzed. Results show that due to a great difference in the viscosity between oil and water phases, the moving interface of water phase is not uniform, and the viscous fingering occurs, tending to proceed along the direction with the minimum flow resistance. There is not a linear relationship between the displacement velocity and the displacement efficiency. Too high displacement velocities do not lead to much better displacement efficiency, while a higher pressure drop is caused. Choosing a proper displacement velocity is indispensable in practical engineering. A lower oil-water viscosity ratio is more favorable to obtain high displacement efficiency. Under the present simulation conditions, when the viscosity ratio is 1.2, the displacement efficiency reaches 96.2% at a moderate Reynolds number. The porosity is not a sole factor determining the displacement performance. Even for the same porosity, the shape and length of preferential flow paths are different and randomly distributed, causing a different displacement performance. A large tortuosity tends to result in a low hydraulic conductivity and displacement efficiency.

Keywords: Sandstone reservoirs; Random pores; Random generation-growth algorithm; Oil-water displacement; Displacement efficiency

Received: 22 Jan 2021/ Accepted: 15 Apr 2021

2305-7068/© 2021 Journal of Groundwater Science and Engineering Editorial Office

Introduction

As a typical kind of fossil energy resources, petroleum is of great importance to maintain industrialized civilization. At present, oil accounts for a large percentage of the world' s energy consumption, around 32% in Europe and Asia and 40% in North America areas (Mirchi et al. 2012; Yang et al. 2013). As regards to oil extraction, one of major methods is water injection, in which the water (e.g. produced water, seawater, groundwater, river water, etc.) is injected to support the pressure of the reservoir and displace oil from the reservoir. Using this method, the production rate of a reservoir can be maintained over a longer period.

During the past decades, a large number of studies have been conducted in order to have an in-depth understanding of the process of oil displacement by using water and to maximally improve the displacement efficiency. Rebold (1962) early presented a method for calculating in-situ values of

*Corresponding author: Hua-jun Wang, *E-mail address*: huajunwang@126.com

DOI: 10.19637/j.cnki.2305-7068.2021.03.006

Gao F, Liu F, Wang HJ. 2021. Numerical modelling of the dynamic process of oil displacement by water in sandstone reservoirs with random pore structures. Journal of Groundwater Science and Engineering, 9(3): 233-244.

oil-displacement efficiency by water flushing using conventional subsurface logs. Rivas-Gomez et al. (2001) simulated the flow behavior within a porous fractured medium where the oil was displaced by water and fractures were represented by channels of 2 mm wide, 1.7 mm deep and 16 cm long; and the water injection rates ranged from 2 mL/h to 200 mL/h, with a variable pressure of between 0.006 and 0.91 psi. Zhao et al. (2002) performed the experiments of water displacing oil in low permeability sandstone reservoirs. Their results showed that different types of fracture had different percolation behaviours and effects on displacement efficiency. The poorer a layer' s permeability was, the lower the layer' s water oil displacement efficiency was. By using visual technology, Sun and Tang (2006) observed that the water injected from the weakly oil-wet to neutral-wet sandstone of low permeability was dominated by the injection pressure. At a low injection pressure, the water can only enter large pores with good hydraulic conductivity. When the injection pressure was increased, water was forced into some small pores to drive oil out. Pore conductivity was critical toward water flooding efficiency in the rocks of low permeability. Fernandez-Berdaguer and Savioli (2009) presented an inverse problem of the displacement of oil by water in porous media, which was used for the estimation of oil−water relative permeability functions. Xu et al. (2011) conducted laboratory experiments to study the pore production characteristics during the water-oil displacement. Their results showed that the remaining oil saturation was high, while the remaining oil was mainly in the small sized pores. During the water-oil displacement, the preferential production pores were super large pores; large and middle pores made great contributions to recovery. The oil displacement efficiency and microcosmic remaining oil distribution were mainly affected by pore structure. Liu et al. (2012) observed the oil and water movement characteristics in the process of water flooding in the network of cracks. They found that residual oil was mainly in the form of isolated droplets, cants and membranes; and the formation and distribution of remaining oil were affected by the wet ability and connectivity of rock cracks. Hossein et al. (2013) made a full review of production prediction models for sandstone reservoirs. Gao and Liu (2013) put forward the heat-driving mechanism in which the movement of the groundwater is caused by the density differences from different temperatures. Lu et al. (2014) presented precise descriptions of saturation, capillary pressure and relative permeability relations for predictions and simulations on multiphase flow system.

In recent years, based on the permeability experiment, Liu (2015) presented a new expression to predict the water-oil displacement efficiency. De Castro and Rodriguez (2015) tested interfacial wave properties of oil-water flow, in which the density and viscosity were 854 kg/m^3 and 300 mPa·s, respectively, and correlated to the flow properties by dimensionless numbers of Reynolds, Froude and Weber. A second-order Fourier series was proposed to model the wave shape, which can be used to predict the geometry and speed of typical oil-water interfacial waves within a wide range of superficial velocities and pipe inclinations. Based on the lattice Boltzmann method, Takeshi et al. (2016) calculated fluid displacements in 3D pore spaces of Berea sandstone and analyzed the effects of capillary number and viscosity ratio on the displacement patterns. They characterized dynamic pore-filling events from the pressure variation of the non-wetting phase, and linked this behavior to the occurrence of capillary fingering. In summary, the actual displacement process is very complex, especially that random pore structures in oil reservoirs have a significant impact on the water-oil movement as well as the displacement efficiency. More recently, Li et al. (2018) performed a simulation of the density change of groundwater flow system in inland basins and found that the increase of fluid density in the central part of the basin would restrain the development of regional groundwater flow system, resulting in a decrease of the circulation rate. Ju et al. (2019) simulated the displacement process of immiscible fluids in a porous structure on the pore scale by using lattice Boltzmann methods, and made an experimental validation using 3D printing technology. Liu et al. (2020) performed physical experiments and numerical simulations of viscosity reducer flooding for ordinary heavy oils. Their results showed that viscosity reducer flooding reduced the starting pressure gradient and the displacement pressure, while the oil recovery factor increased by 12.4% and the total recovery reached 46.6%. Wang et al. (2020) presented a numerical simulation method coupled with dynamic capillary forces, based on the full-implicit method. In short, the above extensive studies provided important insights into the oil-water two-phase flow and a better estimation of flow behavior in oil and gas reservoirs.

In present work, random inner micro-pore structures of sandstone reservoirs will be repro-

duced based on the random generation-growth algorithm. Then, the dynamic process of oil displacement by water will be simulated numerically; and the effects of the displacement velocity, the viscosity ration of oil-water phase and the porosity of oil reservoirs on the displacement efficiency will be analyzed. The present work is expected to provide a useful guide for practical oil-water production engineering.

1 Random generation-growth algorithm for pore structure in reservoirs

For porous media, the random generation-growth (RGG) method is usually designed to reproduce structural assembles of elements with random sizes, locations and orientations, and connections, each of which also grows from randomly distributed seeds and the growth is guided by a few given probabilistic growth rates. For different types of microstructures (e.g. granular, fibrous or netlike), the algorithms will be different but still bear the same principles (Wang and Pan, 2008). In this paper, a multi-parameter random generation-growth method, Quartet Structure Generation Set (QSGS) proposed by Wang and Pan (2008), was used to reproduce the random two phase micro-pore structures of sandstone oil reservoirs, where four parameters were identified in controlling the internal porous structure.

Four parameters include the core distribution probability (c_d), each given directional growth probability (D_i), the porosity (Φ) and phase number (n=2). Detailed algorithms are as follows:

(i) For a random number constrained by a uniform distribution function within (0, 1), if the number is lower than c_d, it will be defined as core.

(ii) For each growing element, new random numbers will be assigned to its neighboring cells. The neighboring cell in direction i will become part of the growing phase if its random number is not greater than D_i. For two-dimensional cases in this paper, each square cell has eight growing directions to its neighbors, as seen in Fig.1. There are four main directions (1-4) and four diagonal directions (5-8). To obtain an isotropic structure in such systems, we set both the main directional growth probabilities $D_{1\text{-}4}$ and the diagonal directional growth probabilities $D_{5\text{-}8}$ into respective constants in each group, and set both constants in a fixed ratio.

(iii) Repeat the growing process of ii) until the volume fraction of the first growing phase reaches the value of porosity Φ.

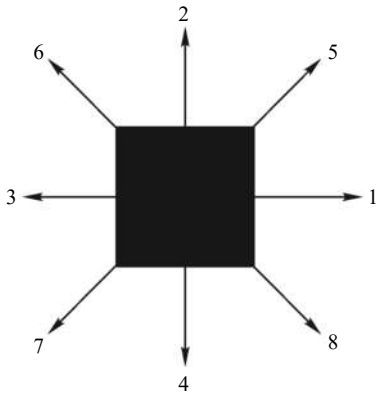

Fig. 1 Eight growth directions of each cell for randomly-generated 2-D porous media

According to previous studies (Wang and Pan, 2008; Wang and Pan, 2009), the parameters are defined as $D_{1\text{-}4}$=1/8, $D_{5\text{-}8}$=1/4, c_d=0.01 for the current study. The random generation and associated visualization of the pore structures of sandstone were conducted by using the MATLAB codes. As an example, Fig. 2 shows the diagram of a typical geometric model for the oil-water displacement simulation. It can be seen in the middle of the porous section that the blue colour is the solid or matrix and the hollow denotes the pore spaces, from which the porosity of oil reservoirs is 0.327. In order to reduce the in-and out-flow effects of seepage at boundaries, the entire computational domain is extended to the dimension of 10 cm long (L) and 4.7 cm wide (W), with its corners marked with A, B, C, and D. Based on this conceptual model, the flow process of oil displacement by water inside the sandstone will be further calculated by the following modelling equation groups.

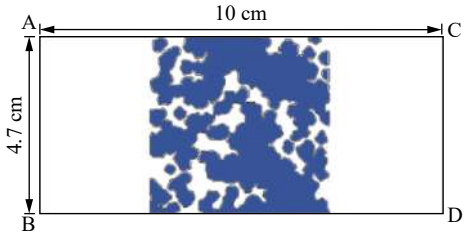

Fig. 2 Diagram of a geometric model for simulation

2 Theoretical model and simulation

2.1 Theoretical models for water-oil mixture phase flow

In this paper, a mixture phase model is used to describe the whole flow process of oil displace-

ment by water in oil reservoirs with the above random pore structures. In this model, the slip velocity among each phase is considered.

Continuity equation of oil-water mixture phase is written as

$$\frac{\partial}{\partial t}(\rho_m) + \nabla \cdot (\rho_m \vec{v}_m) = 0 \tag{1}$$

Where: ρ_m is the density of oil-water mixture (kg/m^3) and $\vec{v}_m$ is the average velocity (m/s). The two parameters can be calculated as follows:

$$\rho_m = \sum_{i=1}^{n} \alpha_k \rho_k \tag{2}$$

$$\vec{v}_m = \frac{\sum_{i=1}^{n} \alpha_k \rho_k \vec{v}_k}{\rho_m} \tag{3}$$

Where: n is the number of phases (i.e. n=2), α_k, ρ_k and $\vec{v}_k$ are the volume fraction (dimensionless), density (kg/m^3) and velocity(m/s) of k^{th} phase, respectively.

Momentum equations of mixture phase is written as

$$\begin{aligned} &\frac{\partial}{\partial t}\left(\rho_m \vec{v}_m\right) + \nabla \cdot \left(\rho_m \vec{v}_m \vec{v}_m\right) = \\ &-\nabla p + \nabla \cdot \left[\mu_m \left(\nabla \vec{v}_m + \nabla \vec{v}_m^{\,T}\right)\right] + \\ &\rho_m g + \nabla \cdot \left(\sum_{i=1}^{n} \alpha_k \rho_k \overrightarrow{v_{dr,k}} \overrightarrow{v_{dr,k}}\right) \end{aligned} \tag{4}$$

Where: μ_m is the viscosity of oil-water mixture (Pa·s), $\overrightarrow{v_{dr,k}}$ is the slip velocity of k$^{\text{th}}$ phase (m/s), and g is the acceleration of gravity (m/s^2).

The viscosity of oil-water mixture and the slip velocity are respectively calculated by

$$\mu_m = \sum_{i=1}^{n} \alpha_k \mu_k \tag{5}$$

$$\overrightarrow{v_{dr,k}} = \vec{v}_k - \vec{v}_m \tag{6}$$

The relative velocity (also referred to as the slip velocity) is defined as the velocity of a secondary phase (p) or oil phase relative to the velocity of the primary phase (q) or water phase:

$$\overrightarrow{v_{qp}} = \vec{v}_p - \vec{v}_q \tag{7}$$

The drift velocity and the relative velocity are connected by the following expression:

$$\overrightarrow{v_{\mathrm{dr},p}} = \overrightarrow{v_{qp}} - \sum_{i=1}^{n} \frac{\alpha_k \rho_k}{\rho_m} \vec{v}_{qk} \tag{8}$$

The volume fraction equation of oil phase is given by

$$\frac{\partial}{\partial t}(\alpha_p \rho_p) + \nabla \cdot (\alpha_p \rho_p \overrightarrow{v_m}) = -\nabla \cdot (\alpha_p \rho_p \overrightarrow{v_{dr,p}}) \tag{9}$$

The Reynolds number (Re) for seepage flow is defined by

$$\mathrm{Re} = \frac{v_w \cdot d}{\mu_w} \tag{10}$$

Where: d is the characteristic size(m, taken as 0.047 m), μ_w is the viscosity of water (m^2/s, taken as 10^{-6} m^2/s). In this case, for example, when the water phase velocity v_w is 3.15e^{-4} m/s, the Re number is calculated as 14.8.

Boundary conditions are given as follows: (i) the upper and lower boundaries are impermeable; (ii) the left boundary is set as the flow inlet; (iii) the right boundary is set as the pressure outlet. For the convenience of analysis, the initial saturation of oil phase is taken as 1.0, although the actual initial saturation in oil reservoirs usually ranges from 0.8 to 1.0.

2.2 Numerical simulation and validation

The above mixture phase model is solved numerically by the software Fluent 6.3. Table 1 shows the major physical parameters for the simulation, where the porosity and density data of sandstone are based on our previous test results. Triangular meshes are applied and the total number of grids is determined as about 430 000 after a grid independence check.

Fig. 3 shows a comparison of the outlet oil phase saturation between the simulation results and experimental data by Li et al. (2006), in which the experimental situations were as follows: i) the porosity of oil reservoirs was 0.346; ii) the density and viscosity of water were 1 000 kg/m^3 and 1.0 mPa·s, respectively; iii) and the density,

Table 1 Major physical parameters for simulation

Item	Unit	Value	Item	Unit	Value
Water density	kg/m^3	1 000	Water viscosity	Pa·s	0.001
Oil density	kg/m^3	900	Oil viscosity	Pa·s	0.048
Sandstone density	kg/m^3	2 500	Sandstone porosity	-	0.327
Surface tension	N/m	0.035	Initial saturation	-	1.0

viscosity and initial saturation of oil phase were 900 kg/m^3, 13.2 mPa·s and 0.809, respectively, as shown in Table 1. It can be seen that under given displacement rate conditions, two results are in good agreement, with the relative error of less than 5%. Therefore, the present pore structure model and simulation method are reliable and suitable for the later analysis.

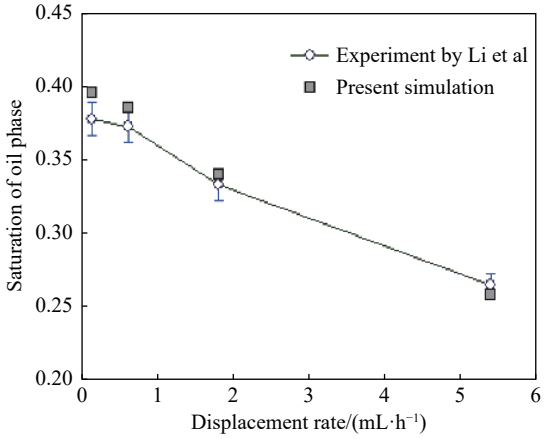

Fig. 3 Comparison of the outlet oil phase saturation between the simulation and experimental results

In order to verify the effects of the size of computational domain, especially the length of left and right boundaries, on the displacement characteristics, two models with different sizes were simulated. As shown in Fig. 4, both cases have the same final saturation of residual oil as well as the displacement efficiency, although a larger length along the flow direction can cause a relatively slow flow and longer period of time to reach a steady state. Table 2 lists the parameters for different simulation situations in the following sections.

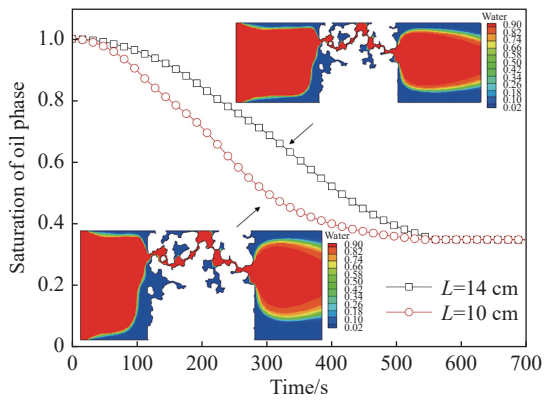

Fig. 4 Comparison of simulation results under different sizes of computational domain

Table 2 Parameters for different simulation situations

No	Porosity	Oil-water viscosity ratio	Re number
1	0.327	48	14.8, 29.4, 58.7, 73.4, 95.4
2	0.327	1.2, 26, 48, 70	58.7
3	0.327, 0.351, 0.384	48	58.7

3 Results and discussion

3.1 Effects of the displacement velocity of water phase

Taking the water phase velocity of 3.15e^{-4} m/s (Re=14.8) as an example, Fig. 5 shows the dynamic distribution of the water phase during the process of oil displacement, where the porosity of oil reservoir and the oil viscosity are 0.327 mPa·s and 4.8 mPa·s, respectively. It can be seen that due to a great difference in the viscosity between oil and water phase, the moving interface of the water phase is not uniform and the viscous fingering occurs. There exists the dominant flow path inside the random pore structures and the seepage flow tends to proceed along the direction with the minimum flow resistance (Meiburg and Homsy, 1988; Flury et al. 1994). In this case, the water phase begins to enter the porous oil reservoir at 120 s and leaves the porous region at 340 s. After 500 s, the whole process of oil displacement reaches a steady state. Because the water phase always flows along the preferential path comprises well connected pores, some of the residual oil inevitably remains in the occluded and dead-end pores that do not contribute to the flow. As a result, the final saturation of the residual oil is only 0.348, namely the displacement efficiency is 65.2%.

Fig. 6(a) shows the variations of the pressure drop between the inlet and outlet under different displacement velocities of water phase, where the porosity of the oil reservoir and the oil viscosity are 0.327 and 4.8 mPa·s, respectively. It can be seen that once the water phase enters the porous oil reservoir, its pressure drops rapidly until the process of oil displacement by water tends to be steady. The higher the velocity of water phase, the shorter the period reaching a steady state of oil displacement is, and the larger the corresponding pressure drop is. For instance, when the velocities of the water phase are 1.25e^{-3} m/s (Re=58.7) and 6.25e^{-4} m/s (Re=29.4), the total pressure drops finally reach 3 817 Pa and 948 Pa, respectively.

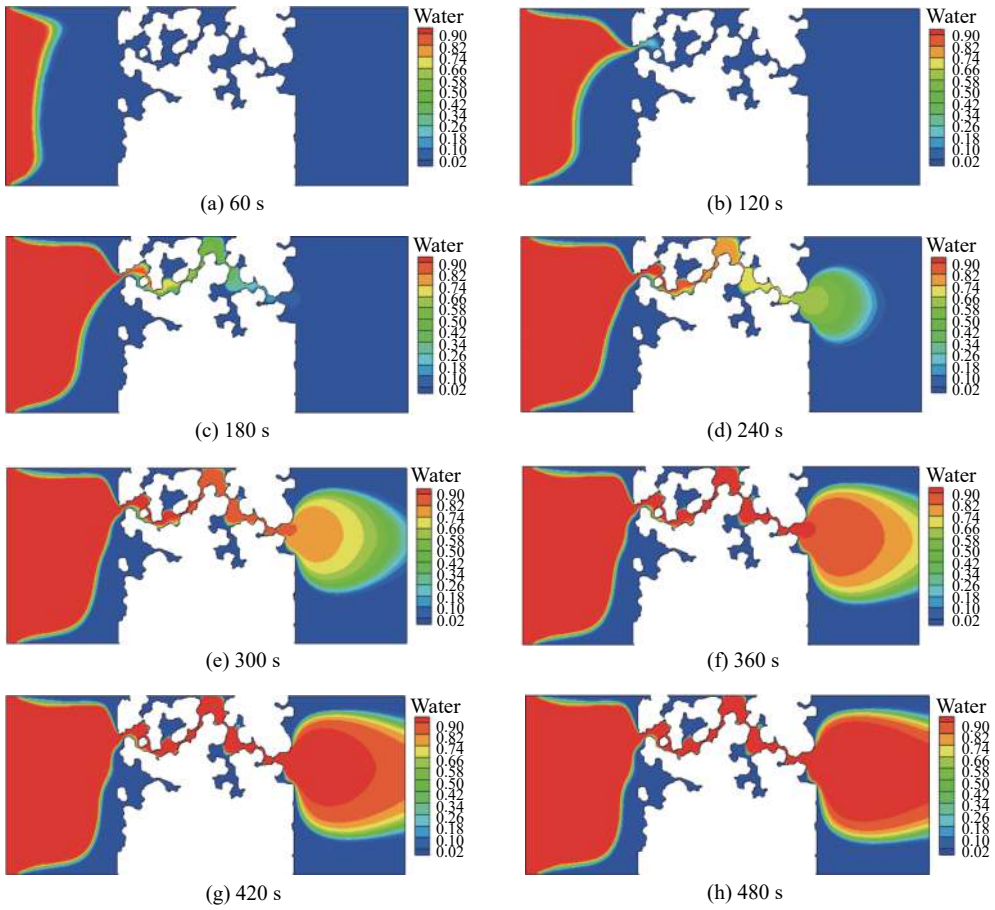

Fig. 5 Distribution of water phase during the process of oil displacement (*Re*=14.8)

Note: The white, red and blue colours represent the matrix of the reservoir, the water phase and the oil phase, respectively, and the transition zone of water-oil phase is shown as the green or yellow colour.

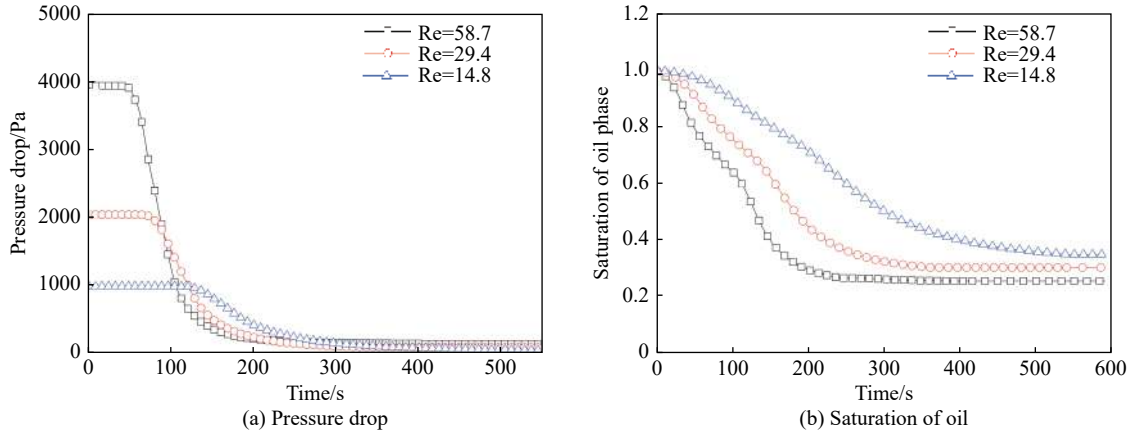

Fig. 6 Variations of the pressure drop and the saturation of oil phase between the inlet and outlet under different displacement velocities of water phase

Fig. 6(b) shows the variations of the saturation of oil phase under different displacement velocities of water phase. It can be seen that as the displacement time increases, the saturation of oil phase drops rapidly and then reaches a relatively steady final saturation. For instance, when the Re numbers are 14.8, 29.4 and 58.7, the corresponding final saturations of residual oil are 0.348, 0.303 and 0.257, respectively. In addition, as the displacement velocities of water phases increase, the time of forming a steady oil distribution becomes shorter. In this case, the above corresponding time lengths are 500 s, 340 s and 240 s, respectively.

Table 3 shows the displacement efficiency under different displacement velocities of water phase. As the Re number increases, the displacement efficiency varies, which follows the regression formula as $DE = 7.3687 \cdot \ln(Re) + 45.0360$. That is to say, as Re increases, the displacement efficiency increases first and then grows slowly until it reaches a steady state. So it can be deduced that a high displacement velocities does not necessarily lead to a good displacement efficiency. On the contrary, a high pressure drop may be caused, thus increasing the energy consumption in transporting the fluid and weakening the economical efficiency of oil production system. Therefore, for the actual process of oil displacement by using water in oil reservoirs, choosing a proper displacement velocity is indispensable (Yang et al. 2013). Generally, the velocity should be determined according to in-situ conditions including pore structures, the viscosity ratio of oil-water, and other factors, which can also be seen in the previous studies (Xu et al. 2011; Liu et al. 2012; Liu, 2015; Takeshi et al. 2016).

3.2 Effects of the viscosity ratio of oil-water phase

Fig. 7(a) shows the variations of the pressure drop between the inlet and outlet under different viscosity ratios (γ) of oil-water phase, where the velocity of water phase is $1.25e^{-3}$ m/s (Re=58.7). It can be seen that for the same velocity of water phase, as the viscosity ratio increases, the pressure drop increases promptly. For instance, when the viscosity ratios are 1.2, 26, 48 and 70, respectively, the total pressure drops are 11 Pa, 1 942 Pa, 3 817 Pa and 5 620 Pa. There is a linear relationship between the total pressure drop and the viscosity ratio, following the regression formula: $\Delta P = 81.842 \cdot \gamma - 123.380$.

Fig. 7(b) shows the variations of the saturation of oil phase under different viscosity ratios of oil-water phase. As the viscosity ratio increases, the final saturation of residual oil also increases and then the displacement efficiency decreases gradually. For instance, when the viscosity ratios are 1.2, 26, 48 and 70, respectively, the displacement efficiencies are 96.2%, 84.7%, 74.3% and 65.7%. Through data regression, the relationship between the displacement efficiency (*DE*) and viscosity ratios (γ) is $DE = 97.238 \cdot \exp(-0.0056 \cdot \gamma) + 45.0360$. From the *DE*- γ relation, it can be inferred that if the viscosity ratio tends to be large enough (e.g. very thick oil), the lowest displacement efficiency would be only 45%. A lower viscosity ratio is hence more favorable for the oil displacement by water and a high displacement efficiency of over 90% can be expected. According to the experiments by Zhang RX et al. (1995), there was no viscous fingering during the process of oil displacement by water at a velocity of $1.17e^{-3}$ m/s (Re=78.3), in which the viscosity ratio and the porosity were 1.0 and 0.215, respectively. As a result, a high displacement efficiency of 92.1% was obtained. On the other hand, according to the experiments by Li et al. (2006), the displacement efficiency was 69.2% at a low velocity of $1.69e^{-4}$ m/s (Re=10.2), where the viscosity of oil was 50 mPa·s (i.e. γ =50) and the

Table 3 Displacement efficiency under different *Re* numbers of water phases

Item	*Re* =14.8	*Re* =29.4	*Re* =58.7	*Re* =73.4	*Re* =95.4
Displacement efficiency(%)	65.2	69.7	74.3	77.0	79.0

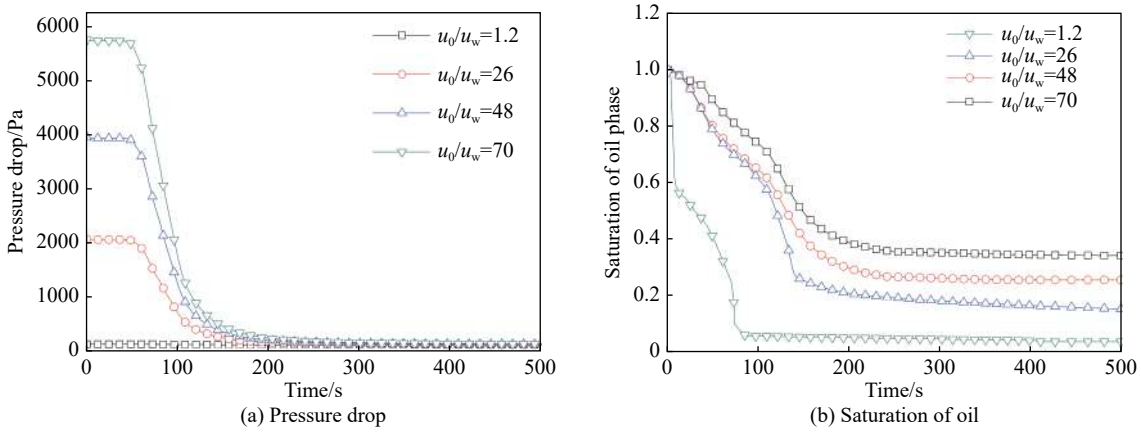

(a) Pressure drop (b) Saturation of oil

Fig. 7 Variations of the pressure drop and the saturation of oil phase between the inlet and outlet under different viscosity ratios of oil-water phase

porosity of oil reservoir was 0.31. By contrast, the present simulation results are in good agreement with the above experimental data, and can be used for the prediction of displacement efficiency in actual oil reservoirs.

Fig. 8 summarizes the variations of the pressure drop and displacement efficiency against the viscosity ratios of oil-water phase. It can also be seen that, for the actual process of oil displacement by water in oil reservoirs, reducing the viscosity ratio of oil-water phase is an important approach to the enhancement of the displacement efficiency (Wei et al. 2013). Usually, the viscosity of oil decreases as its temperature increases. So water with a relatively high temperature is necessary to reduce the viscosity of oil and to improve the final displacement efficiency in reservoirs. For instance, Oliveira et al. (2011) found that for an infinite viscosity ratio, a positive temperature gradient was necessary to enhance recovery. In addition, according to the experiments by Zhang et al. (2017), the irreducible water saturation increased linearly with an increasing temperature, while residual oil saturation decreased nonlinearly with an increasing temperature. In addition, when the temperature increased, both oil and water relative permeability increased under the same water saturation, which indicated that the system became more water-wet. Obviously, this is favorable for the improvement on the displacement efficiency. In practice, this can be done by injecting a hot fluid (e.g. steam or water) into the reservoir, which has been mostly used by companies exploiting heavy oil reservoirs.

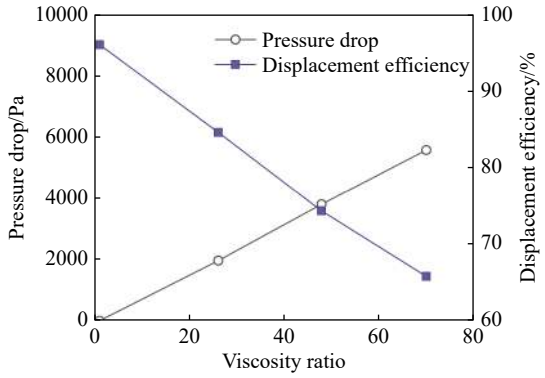

Fig. 8 Variations of the pressure drop and displacement efficiency with oil-water viscosity ratios

3.3 Effects of the porosity of oil reservoir

Fig. 9 shows the distribution of oil phase at 180 s during the process of oil displacement with different porosities of oil reservoirs, where the viscosity ratio of oil-water phase is 48 and the velocity of water phase is $1.25e^{-3}$ m/s (Re=58.7). It can be seen that there is a great difference in the micro-pore structures randomly generated for the porous sandstone oil reservoirs, thereby affecting the process of oil displacement by water. Further, it is not the porosity, but the inner preferential flow path that dominates the final displacement efficiency. For instance, the connectivity of pores in the case of Φ=0.351 is better than that in the cases of both Φ=0.327 and Φ=0.384. The flow velocity at the preferential flow paths is greater than that at other non-dominant flow paths. The existence of such preferential flow paths reflects the complexity and uncertainty of seepage flow inside random porous media in nature. Therefore, even if sandstone oil reservoirs have the same porosity, the shape and length of dominant flow paths are rather different and randomly distributed, thereby causing a different displacement flow characteristics, which will be discussed in the following sections.

Fig. 10 shows the variations of the average velocity of water and oil phases under different porosities. It can be seen that as the displacement proceeds, the average velocities of water phase and oil phase tend to be increasing and decreasing, respectively. In this case, when the porosities of the oil reservoirs are 0.327, 0.351 and 0.384, respectively, the average velocities of oil phase all decrease to near zero at the moments of 220 s, 382 s and 401 s. Compared with the other two cases, the time length of oil displacement is much shorter for the case of Φ=0.327. This is because there is only one narrow preferential flow path, thereby causing much residual oil to be accumulated in those unconnected or closed micro pores. Once these pores are broken through (e.g. by hydraulic fracturing), however, the residual oil will be expected to be released completely and then the displacement efficiency is expected to be further improved.

Fig. 11(a)-(b) show the variations of the pressure drop between the inlet and outlet and the saturation of oil phase under different porosities, respectively. It can be seen that for the same displacement velocity of water phase, the total pressure drop increases as the porosity increases. For instance, when the porosities of oil reservoirs are 0.327, 0.351 and 0.384, respectively, the pressure drops are 3 817 Pa, 4 641 Pa and 5 855 Pa. With respect to the displacement efficiency, due to the effects of preferential flow

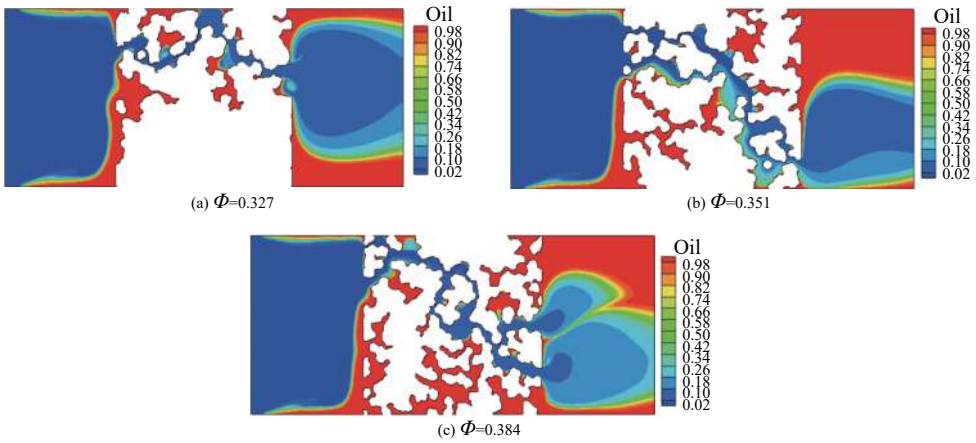

Fig. 9 Distribution of oil phase at 180 s during the process of oil displacement (*Re*=58.7)

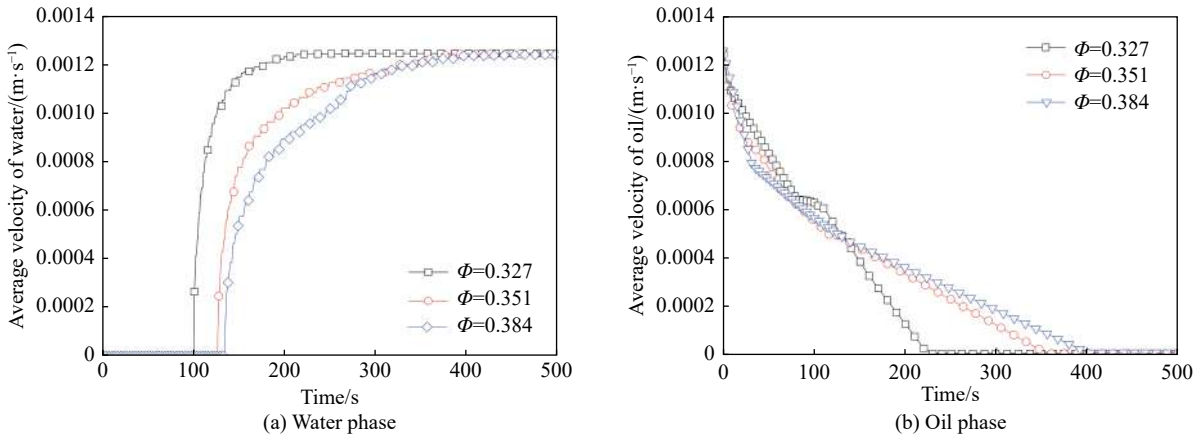

Fig. 10 Variations of the average velocity of water and oil phase under different porosities

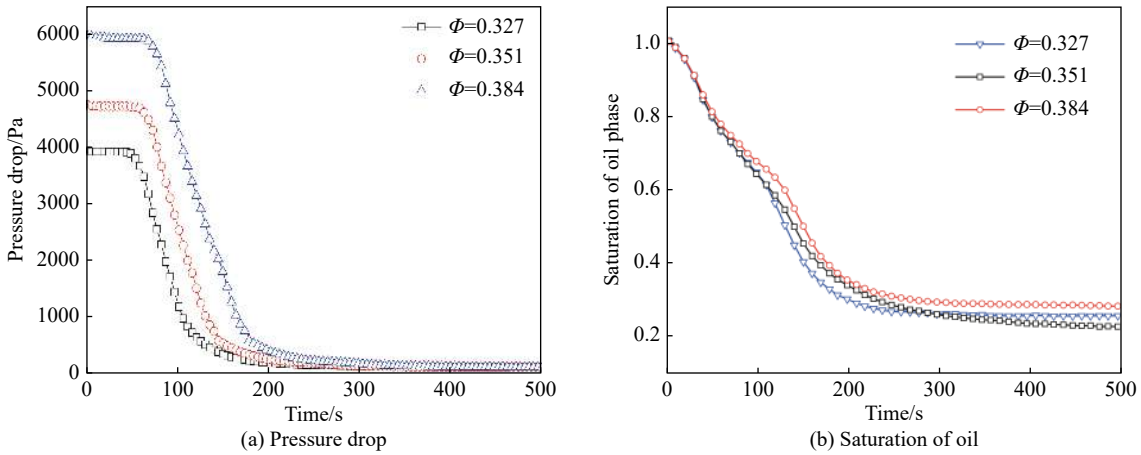

Fig. 11 Variations of the pressure drop and the saturation of oil phase between the inlet and outlet under different porosities

paths in the porous oil reservoirs, the final saturation of residual oil and the displacement efficiency follows the order as Φ=0.351< Φ=0.327< Φ=0.384 and 77.9% >74.4% >71.4%, respectively. Therefore, the porosity is not a sole factor that influences on the displacement performance; and the specific characteristics of micro-pore structures should be taken into full consideration. As shown in Fig. 12(left), for the case of Φ=0.384, the fine throats along preferential flow paths, which is generated randomly by the RGG algorithm mentioned above, are the key localities

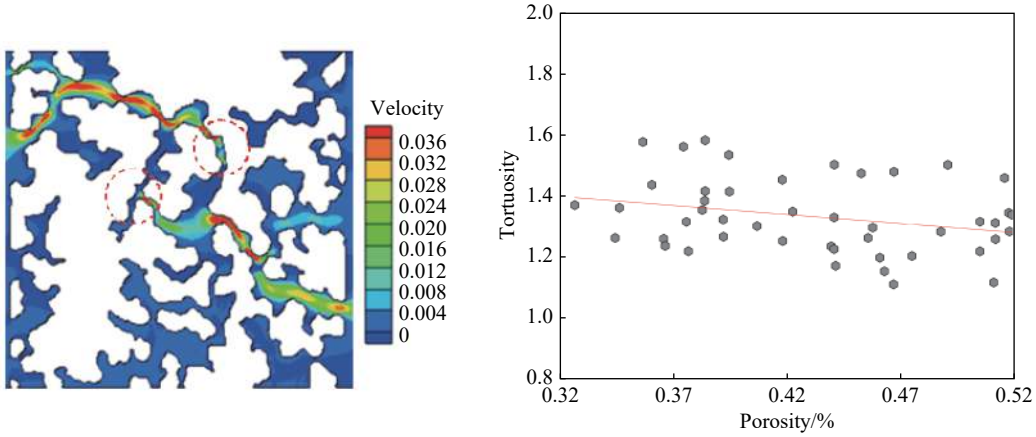

Fig. 12 Fine throats along preferential flow paths (Φ=0.384) and variations of tortuosity with porosity of porous media with random pores

that cause the lower limit of displacement efficiency. In addition, according to the calculation, the hydraulic tortuosities (τ) of the porous region for the case of Φ=0.327 and Φ=0.384 are 1.38 and 1.63, respectively. As an extension, Fig. 12(right) shows the relationship between the tortuosity and the porosity of the porous media with random pores. Notes that the hydraulic tortuosity is often treated as the function of the porosity, where the tortuosity tends to be decreasing as the porosity increases (Koponen et al. 1997; Yang et al. 2016). In fact, this is only valid within a wide range of porosity. For a narrow range of porosity of 0.35±0.03 in the present simulation, however, the above empirical relationship is not valid. Furthermore, even if for the same porosity, its tortuosity is very different due to the random effect. In such a case, the random connectivity of the micro-pore structures is dominated. So a large tortuosity is another major factor resulting in a low hydraulic conductivity and displacement efficiency.

4 Conclusions

In the present work, a number of pore structures of sandstone reservoirs were randomly generated, by using the method of random generation-growth algorithm. On the basis of the conceptually models, the dynamic process of oil displacement by water was then simulated, from which the effects of the displacement velocity, the viscosity ration of oil-water phase and the porosity of reservoirs on the displacement efficiency were respectively analyzed. From the simulated results discussed above, the following conclusions can be obtained:

(1) Due to a great difference in the viscosity between oil and water phases, the moving interface of water phase is not uniform, and the viscous fingering occurs. There exists a dominant flow path inside the random pore structures and the flow tends to proceed along the direction with the minimum flow resistance. Once the water phase enters the porous reservoirs, its pressure and the saturation of oil phase drop rapidly until the displacement process is steady.

(2) As the displacement velocity increases, the displacement efficiency also increases, but there is not a linear relationship. A high displacement velocity does not lead to a good displacement efficiency. On the contrary, a high pressure drop may be caused. For the actual process of oil displacement by using water in oil reservoirs, choosing a proper displacement velocity is critical.

(3) For the same the velocity of water phase, as the viscosity ratio increases, the pressure drop increases linearly, and the final saturation of residual oil increases gradually, too. The increase of viscosity ratio also causes the decrease of the displacement efficiency, of which their relationship can be represented by an exponential function. For the actual process of oil displacement by water in oil reservoirs, a low oil-water viscosity ratio is favorable and a high displacement efficiency of over 90% is expected. Under the present simulation conditions, when the viscosity ratio is 1.2, the displacement efficiency can reach 96.2%.

(4) The porosity is not a sole factor that affects the displacement performance. For random porous reservoirs, there is a great difference in micro-pore structures. Even for the same porosity, the shape and length of dominant flow paths are rather different and randomly distributed, thereby causing different displacement characteristics. A large tortuosity is another major factor resulting in a low

hydraulic conductivity and displacement efficiency.

Acknowledgements

This work was supported by China Geological Survey Program (DD20190128) and Natural Science Foundation of Hebei Province (No. E2019330003).

References

De Castro MS, Rodriguez MH. 2015. Interfacial waves in stratified viscous oil-water flow. Experimental Thermal and Fluid Science, 62: 85-98.

Fernandez-Berdaguer EM, Savioli GB. 2009. An inverse problem arising from the displacement of oil by water in porous media. Applied Numerical Mathematics, 59(10): 2452-2466.

Flury M, Flühler H, Jury W A, et al. 1994. Susceptibility of soils to preferential flow of water: A field study. Water Resources Research, 30(7): 1945-1954.

Gao ZJ, Liu YG. 2013. Groundwater flow driven by heat. Journal of Groundwater Science and Engineering, 1(3): 22-27.

Hossein R, Mahshid J, Saman A, et al. 2013. Review of sand production prediction models. Journal of Petroleum Engineering: 1-16.

Ju Y, Gong WB, Zheng JT. 2019. Characterization of immiscible phase displacement in heterogeneous pore structures: Parallel multicomponent lattice Boltzmann simulation and experimental validation using three-dimensional printing technology. International Journal of Multiphase Flow, 114: 50-65.

Koponen A, Kataja M, Timonen J. 1997. Permeability and effective porosity of porous media. Physical Review E, 56: 3319-3325.

Li LL, Su C, Hao QC, et al. 2018. Numerical simulation of response of groundwater flow system in inland basin to density changes. Journal of Groundwater Science and Engineering, 6(1): 7-17.

Li ZF, He SL, Yang WX, et al. 2006. Physical simulation experiment of water driving by micro-model and fractal features of residual oil distribution. Journal of China University of Petroleum, 30(3): 67-71. (in Chinese)

Liu HH. 2015. New water-oil displacement efficiency prediction method. Open Petroleum Engineering Journal, 7(1): 88-91.

Liu YZ, Sun L, Pan Y, et al. 2012. Experimental study on microscopic water/oil displacement percolation mechanism of fractured reservoir. Reservoir Evaluation and Development, 2(5): 28-31. (in Chinese)

Liu ZP, Wu LG, Wei CP. 2020. Physical experiments and numerical simulations of viscosity reducer flooding for ordinary heavy oil. Journal of Petroleum Science and Engineering, 192: 107194.

Lu C, Li L, Liu YG, Wang GL. 2014. Capillary pressure and relative permeability model uncertainties in simulations of geological CO_2 sequestration. Journal of Groundwater Science and Engineering, 2(2): 1-17.

Meiburg E, Homsy G M. 1988. Nonlinear unstable viscous fingers in Hele–Shaw flows. II. Numerical simulation. Physics of Fluids, 31(3): 429-439.

Mirchi A, Hadian S, Madani K, et al. 2012. World energy balance outlook and OPEC production capacity: Implications for global oil security. Energies, 5(8): 2626-2651.

Oliveira CL, Andrade JS, Herrmann HJ. 2011. Oil displacement through a porous medium with a temperature gradient. Physical Review E Statistical Nonlinear and Soft Matter Physics, 83(2): 648-670.

Rebold JH. 1962. Evaluation of water-oil displacement efficiency using subsurface logs. Journal of Petroleum Technology, 14(1): 17-21.

Rivas-Gomez S, Gonzalez-Guevara JA, Cruz-Hernandez J, et al. 2001. Numerical simulation of oil displacement by water in a vuggy fractured porous medium. Proceedings of SPE Reservoir Simulation Symposium, Houston, Texas.

Sun W, Tang GQ. 2006. Visual study of water injection in low permeable sandstone. Journal of Canadian Petroleum Technology, 45(11): 21-26.

Takeshi Tsuji, Fei Jiang, Kenneth T. 2016. Characterization of immiscible fluid displacement processes with various capillary numbers and viscosity ratios in 3D natural sandstone. Ad-

vances in Water Resources, 95: 3-15.

Wang M, Pan N. 2008. Predictions of effective physical properties of complex multiphase materials. Materials Science and Engineering, 63(1): 1-30.

Wang M, Pan N. 2009. Elastic property of multiphase composites with random microstructures. Journal of Computational Physics, 228: 5978-5988.

Wang SL, Yu CL, Sang GQ, et al. 2020. An oil-water two-phase reservoir numerical simulation coupled with dynamic capillary force based on the full-implicit method. Computers and Mathematics with Applications, 79(9): 2527-2549.

Wei JG, Li AJ, Chen YD. 2013. Oil displacement efficiency and performance evaluation of composite ion profile control agents prepared with oilfield sewage. Advances in Petroleum Exploration and Development, 5(2): 52-57.

Xu CF, Liu HX, Qian GB, et al. 2011. Microcosmic mechanisms of water-oil displacement in conglomerate reservoirs in Karamay Oilfield, NW China. Petroleum Exploration and Development, 38(6): 725-732.

Yang B, Feng LF, Wang S, et al. 2016. A numerical prediction model for hydraulic conductivity of sandy aquifers based on randomly generated pore structures. E. J. Geotechnical Engineering, 21(2): 677-690.

Yang YQ, Cheng LY, Sha O, et al. 2013. Methods of determining oil displacement efficiency of oil displacement agent. Oilfield Chemistry, 30(2): 290-294. (in Chinese)

Zhang LH, Tong J, Xiong Y. 2017. Effect of temperature on the oil-water relative permeability for sandstone reservoirs. International Journal of Heat and Mass Transfer, 105: 535-548.

Zhang RX, Gao YY, Li JM. 1995. Effects of displacement conditions on the water-oil displacement efficiency in glutenite reservoirs. Henan Petroleum, 13(4): 32-37. (in Chinese)

Zhao Y, Qu ZH, Liu Z. 2002. Experimental study on water/oil displacement mechanisms in fractured reservoir by real sandstone micromodels. Petroleum Exploration & Development, 29(1): 116-119. (in Chinese)